Journal of
Materials Chemistry C

Materials for optical, magnetic and electronic devices

Accepted Manuscript

This article can be cited before page numbers have been issued, to do this please use: G. E. Gomez, D. Onna, R. F. D'Vries, B. C. Barja, J. A. Ellena, G. Narda and G. J. D. A. A. Soler-Illia, *J. Mater. Chem. C*, 2020, DOI: 10.1039/D0TC02623A.

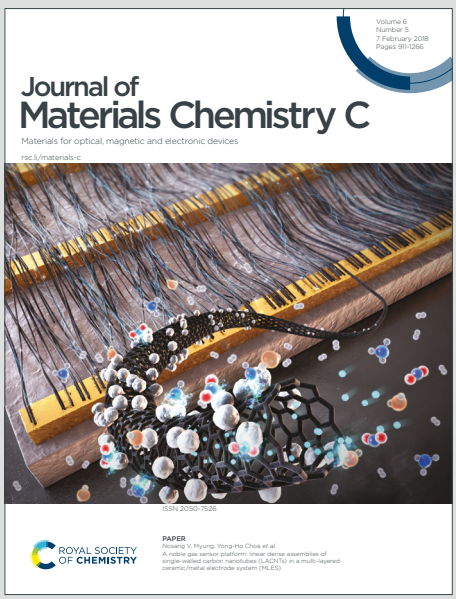

ROYAL SOCIETY OF CHEMISTRY

rsc.li/materials-c

View Article Online
DOI: 10.1039/D0TC02623A

ARTICLE

Chain-like uranyl-coordination polymer as a bright green light emitter for sensing and sunlight driven photocatalysis

Received 00th January 20xx,
Accepted 00th January 20xx

DOI: 10.1039/x0xx00000x

G. E. Gomez,*[a] D. Onna,*[b,c] R. F. D'vries,[d] B. C. Barja,[b] J. Ellena,[e] G. E. Narda[a] and G. J. A. A. Soler-Illia[c]

A new uranyl-coordination polymer (UCP) has been solvothermally synthesized employing succinic acid and 1,10-phenanthroline (phen) as ligands. The obtained compound with formula $[(UO_2)_2(phen)(succ)_{0.5}(OH)(O)_4(\mu_3\text{-}O)(H_2O)]\cdot H_2O$ (**UNSL-1**), is classified as 1D chains showing I^0O^1 connectivity. Also, the asymmetric unit is composed by two hepta-coordinated uranyl centers: U1 surrounded by five oxygen atoms from succinate, meanwhile U2 surrounded by two nitrogen atoms from phen and three oxygen atoms from succinate ($[U1O_7]$ and $[U2N_2O_5]$). The Secondary-Building Unit (SBU) is composed by a sharing edge tetrameric cluster linked by succinate ligand in the [-1 0 1] direction. Besides, the chains are reinforced by π-π stacking interactions from between the aromatic rings of phen molecules to conform a 2D supramolecular arrangement. Moreover, photoluminescence experiments show strong green emission consistent with uranyl crystalline materials. The photophysical characterization was completed by low-temperature measurements (77 K) and recording the decay emission for calculating the lifetime (τ_{obs}) value. Regarding its multifunctional properties, a cation-sensing performance was achieved founding selective quenching toward iron ions in aqueous media. Finally, **UNSL-1** was tested as an efficient water photocatalyst of dye degradation under simulated sunlight irradiation, exhibiting promising results for organic-pollutant water remediation.

1. Introduction

The study of the crystalline uranyl–coordination polymer (UCPs) has been intensively explored in the last decade, mainly due to its potential applications and the variety of novel achieved architectures.[1] Furthermore, the rational combination of organic ligands together with the coordination modes of the uranyl cation $[UO_2]^{2+}$ has led to the formation of an important number of new organic–inorganic connectivities with different dimensionalities and nuclearity of uranyl centred building units.[2] These crystalline assemblies are commonly obtained by employing O-donor molecules such as polycarboxylic acids. Nevertheless, the use of N-donor auxiliary ligands such as aromatic amines gives rise to unpredictable architectures such as isolated clusters, chains, layers, rings, multicavity-structures among others.[1]

In this sense, recently were obtained a set of 0D and 3D luminescent UCPs employing a combination of 2,2′-bipyridine-3,3′-dicarboxylic acid and 2,2′:6′,2″-terpyridine ligands and d-block elements, obtaining a new 9-nodal 3,3,3,3,3,3,3,4,5-connected network, denoted as *geg1* topology.[3]

Since the succinate linker (succ) has the particularity of being a flexible ligand, it can adopt different conformations when it is coordinated by a metal center under determined kinetic and thermodynamic conditions.[4] The interest in succinate-based coordination polymers has been a motivation for the exploration of structures employing lanthanides[4] and actinides.[5] In addition, from the crystal designing point of view, N-ancillary ligands such phenanthroline-like molecules, have shown antenna effect properties in photoluminescence (PL) for a variety of f-elements[6,7] based structures. A summary of all the UCPs obtained by employing succinate ligand is depicted in Table 1.

Moreover, due to the water-stability and the accessibility to active 5f-centers, it was demonstrated the photocatalytic performance of UCPs towards the removal of organic pollutants UV/visible/UV-visible irradiation from wastewater becoming a novel option for the traditional photocatalysts such TiO_2 or ZnO.[8]

Herein, a one-dimensional mixed UCP constructed by using succinic acid and 1,10-phenanthroline, $[(UO_2)_2(phen)(succ)_{0.5}(OH)(\mu_3\text{-}O)(H_2O)]\cdot H_2O$, (namely from now as **UNSL-1**) has been synthesized *via* the solvothermal method. The compound was structurally characterized by single-crystal X-ray diffraction and thermal properties were analysed. Since **UNSL-1** exhibited a bright green emission derived from the uranyl transitions, it was used as multifunctional optical material. In this sense, **UNSL-1** was tested as a chemical-sensor for cations in aqueous media. Finally, its photocatalytic performance for Methylene blue (MB) degradation was studied under Xenon lamp as simulated sunlight irradiation. These exciting results open up the use of actinide-derivate compounds for potential environmental applications.

[a] Instituto de Investigaciones en Tecnología Química (INTEQUI), Área de Química General e Inorgánica, Facultad de Química, Bioquímica y Farmacia, Chacabuco y Pedernera, Universidad Nacional de San Luis, Almirante Brown, 1455, 5700 San Luis, Argentina. E-mail: gegomez@unsl.edu.ar
[b] Instituto de Química, Física de los Materiales, Medioambiente y Energía (INQUIMAE-CONICET), DQIAQF, Universidad de Buenos Aires, Ciudad Universitaria, C1428EHA-Buenos Aires, Buenos Aires, Argentina. E-mail:diego.onna@qi.fcen.uba.ar
[c] Instituto de Nanosistemas, Universidad Nacional de San Martín (INS-UNSAM), Av. 25 de Mayo 1021, San Martín, Buenos Aires, Argentina.
[d] Universidad Santiago de Cali, Calle 5 # 62-00, Cali, Colombia.
[e] Instituto de Física de São Carlos, Universidade de São Paulo, A. Trabalhador São-carlense, nº 400 Parque Arnold Schimidt, São Carlos, São Paulo, 13566-590, Brazil.

Electronic Supplementary Information (ESI) available: PXRD profile, decay emission fitting data, diffuse reflectance spectrum, and emission spectra from sensing experiments. Reference number 1941819 contains the supplementary crystallographic data for this work. This data can be obtained free from the Cambridge Crystallographic Data Centre via: www.ccdc.cam.ac.uk/data_request/cif. See DOI: 10.1039/x0xx00000x

Table 1. Summary of UCPs constructed by using succ ligand.

UCP "succinte types"	crystalline architecture features				Properties	Ref.
	I^nO^m	Space group	U^{VI} CN	SBU		
$[(UO_2)(succ)(H_2O)]$	I^0O^3	Ama2	7	chain	PL and photocatalysis	5d
$[(UO_2)(succ)_{1.5}]\cdot(bipy)_{0.5}\cdot(succ)_{0.5}\cdot 3H_2O$	I^0O^2	C2/c	8	layer	PL and photocatalysis	5d
$[(UO_2)(succ)]\cdot H_2O$	I^0O^3	$P2_1/n$	7	chain	no reported	5a
$[(UO_2)_2(phen)(succ)_{0.5}(OH)(\mu_3\text{-}O)(H_2O)]\cdot H_2O$ **(UNSL-1)**	I^0O^1	Pī	7	chain	PL, τ_{obs}, sensing and photocatalysis	this work
$K_2[(UO_2)_2(succ)_3]$	I^0O^2	$I\,4_1/a$	8	layer	no reported	5c
$[Mg(H_2O)_6][(UO_2)_2(succ)_3]\cdot 2H_2O$	I^0O^1	Pī	8	chain	no reported	5c
$[(UO_2)_4(succ)_2(Hsucc)_4]\cdot 2H_2O$	I^0O^3	P32	7 and 8	chain	PL	5b

Experimental Section

1.1. Synthesis:

Caution! *Although the uranyl nitrate hexahydrate ($UO_2(NO_3)_2\cdot 6H_2O$) used in these studies contains depleted uranium, standard precautions for handling radioactive and toxic substances should be followed*.

All materials, including succinic acid (H_2succ), 1,10-phenanthroline (phen), were purchased from SIGMA-ALDRICH and used without further purification. 0.33 mmoles (0.15 g) of $UO_2(NO_3)_2\cdot 6H_2O$, 0.33 mmoles (0.06 g) of phen and 0.33 mmoles (0.036 g) of H_2succ were mixed in water: o-xylene (6:3). Also, 0.625 mL of 5 M of NaOH solution was added in order to reach a final pH of 6.5. Then the cloudy yellowish mixture was stirred at 500 rpm for one hour at room temperature. After that, the mixture was carefully transferred to 45 mL Teflon-lined Parr autoclave at 140 ºC for 72 hours. The obtained yellow crystalline product was washed three times with water and o-xylene and dried at room temperature. Yield: 43% (based on U).

1.2. UV-Vis Absorption Spectroscopy

UV-Vis Absorption Spectra were recorded with a Shimadzu UV-3600 Plus with quartz cuvettes (Shimadzu, Japan).

1.3. Diffuse Reflectance Spectroscopy

Reflectance Spectra were recorded with a SD2000 Miniature Fiber Optic Spectrometer detector from Ocean Optics, using a tungsten halogen light source (HL-2000-LL) and an ISP-50-8-R-GT integrating sphere.

1.4. Thermal Analysis

Thermogravimetric Analysis (TGA) was performed with a TA Instruments – TGA Q500 apparatus under air flux (100 ml min^{-1}), in alumina pans heated up to 800 °C at a heating rate of 10 °C min^{-1} rate.

1.5. Powder X-ray diffraction (PXRD)

The PXRD pattern was obtained with a Rigaku ULTIMA IV diffractometer using CuKα radiation (λ1= 1.54056 Å, λ2= 1.54439 Å) (see ESI section S1).

1.6. Single-Crystal structure determination (SCXRD)

SCXRD data for **UNSL-1** were collected at room temperature (293(2) K) on a Rigaku XTALAB-MINI diffractometer using MoKα radiation (0.71073 Å) monochromated by graphite. The cell determination and the final cell parameters were obtained on all reflections using the software CrysAlisPro.[9] Data integration and scaling procedures were carried out using the software CrysAlisPro.[9] The structure were solved and refined with SHELXT[10] software, and refined using full-matrix least-squares method within SHELXL software,[11] included in WinGX[12] and Olex2.[13] Non-hydrogen atoms were clearly resolved and full-matrix least-squares refinements of these atoms with anisotropic thermal parameters were performed. Besides, hydrogen atoms were stereochemically positioned and refined by using the riding model.[10] ORTEP diagrams for all structures were prepared with Diamond.[14] TOPOS[15] and Mercury[16] programs were used in the preparation of the artwork of the polyhedral and topological representations.

1.7. Luminescence Measurements

The solid-state luminescence measurements were performed on a PTI QuantaMaster QM-1 luminescence spectrometer. A 75 W Xenon lamp was used as the excitation source. The excitation–emission spectra were measured in the solid state at 77 and 298 K. The steady state luminescence of the suspension and lifetime measurements were performed on an Edinburgh Instruments FS5 Spectrofluorometer equipped with both continuous (150 W) and pulsed xenon lamps. Prior to the PL studies, the sample was ultrasonicated at 80 KHz for 10 minutes for obtaining a homogeneous suspension. Excitation spectra were corrected for the xenon lamp emission profile, whereas emission spectra were corrected for the detector response curve. The data were collected at every nanometer with an integration time of 0.2 seconds for each step.

1.8. Sensing

The sensing activity of **UNSL-1** was tested, by monitoring the emission spectra at 515 nm at an excitation wavelength of 365 nm. Firstly, the suspension emission and then in presence of a set of 200 ppm of monovalent and divalent ions solutions (Mn^{2+}, Ni^{2+}, Mg^{2+}, Zn^{2+}, Ba^{2+}, Na^{+}, Co^{2+}, Cd^{2+}, Ca^{2+}, Hg^{2+}, Sr^{2+}, K^{+}, Cu^{2+} and Fe^{2+}) were measured. These samples were 2 mL suspensions of **UNSL-1** in water (0.4 mg · mL^{-1}).

Note: The solutions were freshly prepared in a volumetric flask before used in order to avoid any contamination or oxidation.

1.9. Photocatalysis

UNSL-1 was dispersed in water using an ultrasonic bath of 40 kHz in a proportion ca. 1 g · L^{-1}. Then, an aliquot of Methylene-Blue (MB) was added up to 40 ppm concentration and this suspension was stirred in the dark for 30 min to reach equilibrium. MB degradation experiments were performed for 100 min on stirred solutions in quartz cells at room temperature. During irradiation, aliquots from the suspension were taken from the reaction cell at 10, 20, 30, 40, 60 and 100 min. The reaction was measured as a function of time by recording the UV–vis spectra of the remaining MB using an Ocean Optics modular spectrometer (SD2000).

The photocatalysis was performed under a 150 W XBO Osram Xe lamp. The light was filtered using a $CuSO_4$ solution (an IR filter) for

minimizing the sample heating. This configuration with continuum emission between 400 and 600 nm and 2700 μW·cm^{-2} (λ_{max} = 520 nm) irradiance is referred to as sunlight-like irradiation.[17] The Xe lamp spectrum in this configuration could be found elsewhere.[16]

2. Results and discussion

2.1. Crystal structure of UNSL-1.

Under solvothermal conditions, needle shape crystals suitable for single crystal X-ray diffraction were obtained. The compound crystallizes in the triclinic Pī space group meanwhile the cell parameters and refinement statistics are shown in Table 2.

Table 2. Single crystal X-ray diffraction parameters data for **UNSL-1**.

	UNSL-1
Emp. Formula	$C_{14}H_{15}O_{10}N_2U_2$
FW (g·mol^{-1})	847.34
Temp. (K)	293(2)
λ (Å)	0.71073
Crystal system	Triclinic
Space Group	Pī
Unit cell	
a (Å)	7.7476(7)
b (Å)	10.9968(9)
c (Å)	11.7793(10)
α(˚)	87.274(7)
β (˚)	75.744(7)
γ(˚)	84.385(7)
Volume (Å^3)	967.72(15)
Z	2
ρ $_{calcd}$ (mg·m^{-3})	2.908
Abs. Coeff (mm^{-1})	16.768
F(000)	754
θ range (˚)	2.5 to 34.3
Collected reflections / Unique [R(int)]	24214/7560 [0.031]
Completeness (%)	99 %
Data / restraints / parameters	7560/0/255
Gof on F^2	1.06
R1 [I>2σ(I)]	0.0273
wR2[I>2σ(I)]	0.0619

As is shown in Figure 1, the asymmetric unit of **UNSL-1** consists of two crystallographically independent $[UO_2]^{2+}$ centres exhibiting a pentagonal bipyramidal distorted polyhedra geometry (PBPY-7, Figure 2).[18] The metal centers represent the corresponding Primary-Building Units (PBUs) of the present crystalline structure.

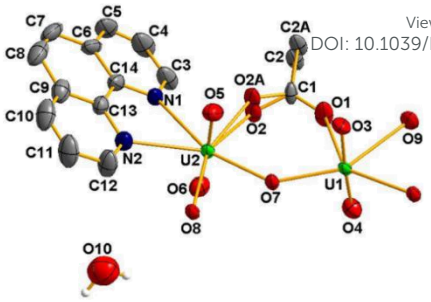

Figure 1. ORTEP representation of the asymmetric unit of **UNSL-1**; ellipsoids are displayed at the 50% probability level.

As is shown in the Figure 2a, U1 presents an [U1O$_7$] environment formed by two axial "yl" oxygen atoms (O=U=O), two μ_3-O atoms, one μ-OH anion, one water molecule and one oxygen atom from the carboxylate group. In the U2 case (Figure 2a), the [U2N$_2$O$_5$] environment is formed by two nitrogen atoms from the phen molecule, two "yl" oxygen atoms, one μ_3-O atom, one μ-OH anion and one oxygen atom from the carboxylate group.

Besides, the secondary building units (SBU) is formed by a sharing edge tetrameric cluster noted as $[U_4(\mu_3\text{-}O)_2(\mu\text{-}OH)_2(H_2O)_2(O_{cb})_4]$ (cb = carboxylate).

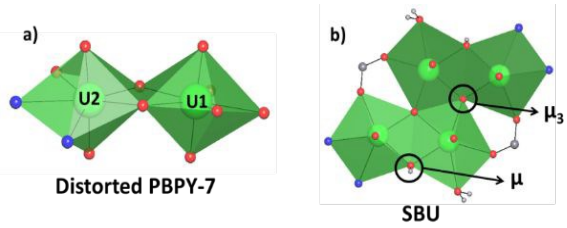

Figure 2. Polyhedra representation of the uranium PBUs (a) and the tetramer uranium SBU (b) in the **UNSL-1** compound.

The succ ligand, in a *trans*-conformation, links two SBUs through μ-carboxylate group giving rise infinite chains growing along [-1 0 1] direction (Figure 3). The polymeric chains exhibit hydrogen bond interactions along [1 0 0] direction between the water molecule and hydroxyl group showing distances of O8···O3 = 2.880(2) Å and O9···O6 = 2.854(2) Å, respectively (Figure 4a). The hydrogen bond distances are displayed in ESI, section 2.

Also, the lattice water molecule plays an important structural role by reinforcing the chains through hydrogen bond interactions with "yl"-oxygen atoms exhibiting O10(w)···O3 = 2.840(3) Å and O10(w)···O4 3.004(4) Å distances. Besides, a hydrogen interaction between coordinated and free water molecules with a O10(w)···O9(w) distance of 2.863(4) Å, was observed. The "key" role of lattice water molecules in the reinforcement of low dimensional frameworks has been previously studied in layered lanthanide compounds.[19]

Finally, the 3D supramolecular structure is formed by π-π stacking interactions between the aromatic rings of phen molecules in "face-to-face" fashion belonging two adjacent chains (centroid···centroid distance= 3.750(3) Å) along [1 1 1] direction (Figure 4b).

Basing on both organic connectivity between metal centres and extended inorganic connectivity, **UNSL-1** can be classified as I^0O^1 type of crystalline structure. According to this nomenclature,[20] I^0 means that the inorganic connectivity is 0 D and O^1 implies that the

organic one is 1D, which involves organic succ linkers connecting the SBUs in one crystallographic direction; the sum of the exponents gives the overall dimensionality of the structure.

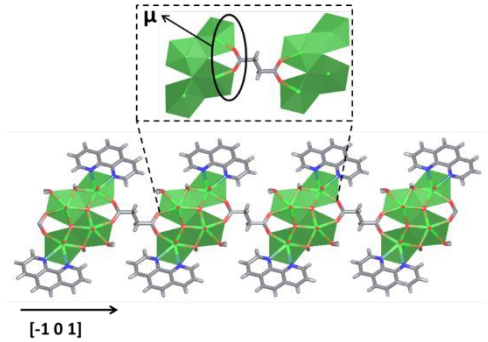

Figure 3. View of the infinite chains along [-1 0 1] direction. The insight shows the connectivity of two adjacent SBUs by the *trans*-succ ligand.

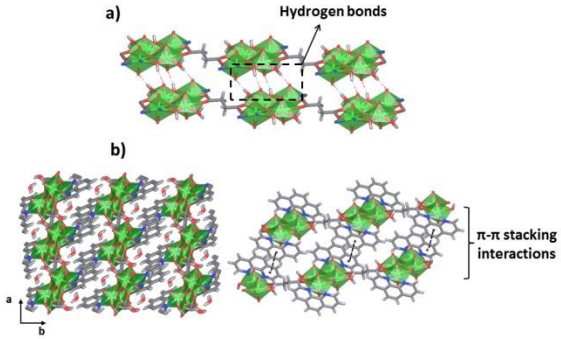

Figure 4. View along [1 -1 1] direction of the hydrogen bond interactions between the polymeric chains (a). Crystal packing view in the plane (0 0 1) and the π-π stacking interactions (b).

2.2. Thermal and vibrational behaviour.

Thermogravimetric analysis was carried out on **UNSL-1** to elucidate the thermal stability, being a parameter for its use in many applications. The initial mass loss step is ascribed to lattice and coordinated water molecules (exp: 4.2%, cld.: 4.24%) in the range of 35-245 °C. Significant mass loss occurs after 320 °C (exp. 33.5% and cld. 33.8 %) which is related to the final decomposition of the succ and phen ligands. It is important to highlight that many 3D MOFs are reported to have a thermal stability regime into the 300−400 °C range, which is comparable to that of **UNSL-1** compound, however, some traditional crystalline structures are more stable to slightly higher temperatures (>400°C).[21] The water loss and organic decomposition were confirmed by mass spectroscopy technique, by detecting the mass ions 18 (H_2O) and 44 m/z (CO_2) respectively (see ESI, section 3).

2.3. Photoluminescence studies.

Collecting photoluminescence spectra and calculating the decay lifetimes (τ_{obs}) of **UNSL-1** seems to be a representative way to explore the structure-property relationships of the optical behaviour of a metal-hybrid material.[22]

Uranyl emission is originated from a ligand to metal charge transfer (LMCT) that excites an electron from nonbonding $5f_\delta$, $5f_\phi$ uranyl orbitals to uranyl− oxygen bonding orbitals (σ_u, σ_g, π_u, π_g),[23] which is further coupled to "yl" vibrational ($S_{11} \rightarrow S_{01}$ and $S_{10} \rightarrow S_{0v}$ [v = 0−4]) states of the U=O axial bond.[24] This emission is often characterized by green emission, observed as four to six vibronically coupled peaks (up to 12) in the 400−650 nm range.[25,26,27]

Figure 5 shows the emission and excitation spectra of **UNSL-1** in solid-state and in aqueous suspensions. By monitoring the emission at 506 nm, broad excitation bands are achieved which are attributed to a combination of phen ligand accompanied by the typical uranyl bands.[22] By exciting the **UNSL-1** (λ_{exc}= 325 nm) at 298 K into the LMCT bands, a broad emission band centred at 320 nm from uranyl transitions is observed in solid-state. In addition, the same sample measured at 77 K shows a more detailed structured spectrum, where the fine uranyl transitions located in the 450-600 nm range (see Figure 5a) give rise to a bright green emission. The emission intensity is enhanced as decreasing the temperature, due to the deactivation of nonradiative-decay.[2] At 298 K the excitation spectra (λ_{exc}= 365 nm) of the aqueous suspensions present two bands: (i) 275 – 375 nm, which corresponds to a LMCT band and (ii) 375 – 450 nm, which corresponds to uranyl bands (Figure 5b). The emission spectra present a broad band with a maximum at 515 nm caused by the interaction of **UNSL-1** with the solvent.

The emission performance was carried out by calculating the CIE x,y coordinates (Commission Internationale de l'éclairage) in both, solid-state and aqueous suspension (Figure 6). Nevertheless, the broad spectrum shape suggests the inhomogeneity environment of uranyl centres due to two different types of polyhedra found in **UNSL-1** structure (Figure 2).

This compound exhibited well-structured metal-centred emission that is enhanced by the sensitization process of the phen molecules coordinated to uranyl centres. For an efficient energy transfer, the energy gap between the triplet state energy of the ligand ($^3T^*$) and the resonant level of "f" element ions, ($^3T^*$-Ln^{3+}),[28] must be in the 3000±500 cm^{-1} range. The triplet states ($^3T^*$) of phen (22100 cm^{-1})[29] matches well with the emissive level of $[UO_2]^{2+}$ (21321 cm^{-1}),[30] demonstrating that an energy transfer process is feasible.

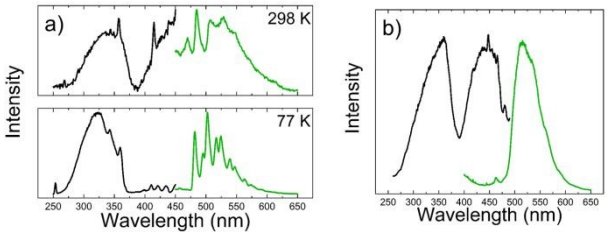

Figure 5. Excitation (black trace) and emission spectra (green trace) of **UNSL-1** in (a) solid-state and (b) aqueous suspension. Excitation spectra were monitored at 506 nm and the emission spectra were excited at 323 nm for solid-state, and 515 nm and 365 nm for aqueous suspension respectively.

Moreover, time-resolved data of **UNSL-1** were collected at an excitation wavelength of 365 nm monitoring the emission at 515 nm (ESI, section 5). The resulting biexponential fitting (R^2= 0.999) (equation 1) revealed two lifetimes (τ_{obs}) values of 14.3 μs and 4.4 μs.

$$I = A + I_1.e^{-t/\tau_1} + I_2.e^{-t/\tau_2} \quad (1)$$

This model suggests the presence of two different emitting centers in the material, which is consistent with the information from the crystalline structure having [U1O$_7$] and the [U2N$_2$O$_5$] uranyl PBUs. This behaviour can be explained as the lifetime of $[UO_2]^{2+}$ group is affected by its chemical environment (lattice solvent, type of PBU, SBU connectivity, etc).[3]

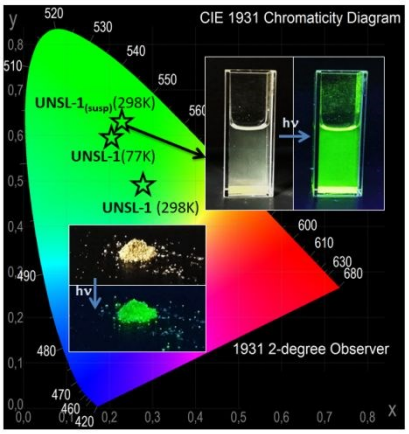

Figure 6. CIE x,y chromaticity of **UNSL-1** compound in suspension and solid state (77 and 298 K).

2.4. Sensing studies.

In the context of chemical sensing, Tb^{3+}/Eu^{3+}-MOFs have been studied as suitable platforms due to their 4f hypersensitive transitions which are affected by the physical[31,32] and chemical[33,34,35] environment. Nevertheless, the use of actinide-compounds in this field is scarce and not much explored by the MOF community.

In order to investigate potential sensing applications, the luminescence of **UNSL-1** was monitored in aqueous media in the presence of a set of monovalent and divalent ions solutions (Mn^{2+}, Ni^{2+}, Mg^{2+}, Zn^{2+}, Ba^{2+}, Na^{+}, Co^{2+}, Cd^{2+}, Ca^{2+}, Hg^{2+}, Sr^{2+}, K^{+}, Cu^{2+}, and Fe^{2+}) at a fixed 200 ppm concentration. Finely ground powder of **UNSL-1** was dispersed into 2 mL of metal aqueous solutions. After sonicating for 30 minutes, the emission spectra were collected (λ_{exc}=365 nm) under stirring.

For a quantitative study, fluorescence measurements were carried out as it is detailed in the Experimental Section 1.8.

A broad band assigned to uranyl transitions $S_{10} \rightarrow S_{0v}$ (v = 0-4) is observed. Differences in intensity values have been seen in the sets of emission spectra (ESI section 6). Indeed, the uranyl transition intensity depends on the cationic specie, being affected by a quenching effect particularly in the presence of Fe^{2+}. It is worth noticing that the solutions were freshly prepared and the Fe^{2+} oxidation kinetic is slow enough to ensure no significant amount of Fe^{3+} is formed.[36] In addition, the absorbance spectra of Fe^{2+} solution, shown in ESI section 6, exhibited a typical band around 300 nm.[37] Finally, the quenching coefficient of uranyl with Fe^{3+} is 3 orders smaller than with Fe^{2+}.[38,39] These facts explain the sensibility towards Fe^{2+}.

When the luminescence of **UNSL-1** is recorded into the 0-25.5 mM [Fe^{2+}] range, a quenching of ~75% is achieved (Figure 7a). In a first approximation, the quenching effect of iron was modelled according to a Stern-Volmer's law[40,41] employing the equation 2.

$$I_0/I = 1 + K_{SV} \cdot [Fe^{2+}] \quad (2)$$

In this equation, I_0 and I indicate the luminescent intensities of **UNSL-1** before and after being exposed to different Fe^{2+} concentrations respectively, with K_{SV} the quenching coefficient (0.077±0.004 mM^{-1}). From the linear fitting (R^2=0.98), it was possible to estimate the limit of detection (LOD) and the limit of quantification (LOQ) using the equations presented in ESI section 8. These values were 2.2 and 7.5 mM respectively. For comparative purposes, the PL response of **UNSL-1** was monitored under the same concentration range of Co^{2+} to demonstrate that no changes in intensities were detected (Figure 7c and 7d). The most plausible reason for quenching could be attributed to charge transfer from Fe^{2+},[38,39] but we cannot discard energy transfer paths considering that the absorbance of Fe^{2+} solution exhibits partial overlapping with the **UNSL-1** spectra that could hinder the emission in some degree, as shown in ESI section 7.

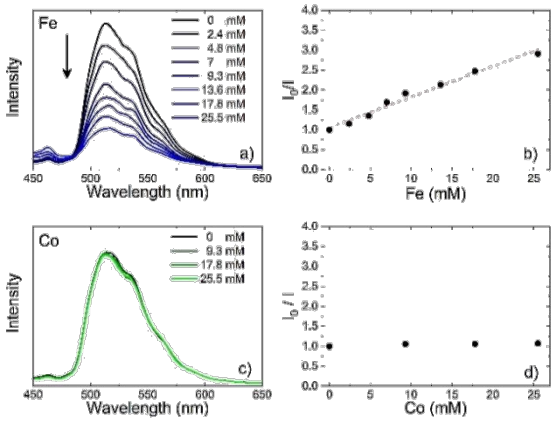

Figure 7. Emission spectra (a) and the relative intensity (b) of **UNSL-1** into the Fe^{2+} 0-25.5 mM concentration range. Emission spectra (c) and the relative intensity (d) of **UNSL-1** into the Co^{2+} 0-25.5 mM concentration range.

2.5. Photocatalysis studies.

Specific studies have demonstrated that aqueous solutions of $[UO_2]^{2+}$ ions were photocatalytically active towards the oxidation of organic substrates in presence of air, but at the same time, it was hard to separate the $[UO_2]^{2+}$ ions from the reaction systems, which hindered this catalyst for practical application.[42] Then, by using a solid containing uranyl species could increase the separation of $[UO_2]^{2+}$ ions.

Due to the insolubility of **UNSL-1** compound in water; the photocatalytic activities of the as-prepared material were investigated. Methylene-blue (MB), an organic pollutant difficult to degrade, was selected as the model of dye under sunlight irradiation. The change in the concentration of MB was analysed by measuring its maximum absorbance located at 665 nm for 100 minutes (see Figure 8a). The MB concentration ratio (C/C_0) shows a decrease of 64 % in 100 min (Figure 8b, **UNSL-1 + MB + hν**).

Also, two control experiments were carried out in order to confirm the photocatalytic activity of **UNSL-1**. One consisted of a MB suspension containing ca. 1 $g{\cdot}L^{-1}$ of finely powdered **UNSL-1** without light assistance and stirred till 100 min. After that, no intensity decrease was achieved in the set of absorption spectra (**UNSL-1 + MB**). Secondly, the direct photolysis of MB without **UNSL-1** was studied for comparison by sunlight-like irradiation, and no changes in intensity were observed for the irradiation time of 100 min (**MB + hν**).

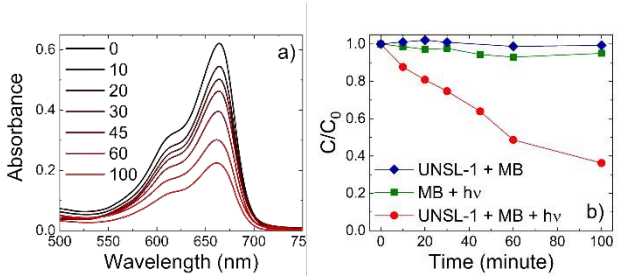

Figure 8. Absorption spectra of MB solution monitored during the photocatalysis reaction employing **UNSL-1** (a). Relative concentration (C/C_0) of MB as a function of time when irradiated under sunlight-like using **UNSL-1** as photocatalyst and its controls (b).

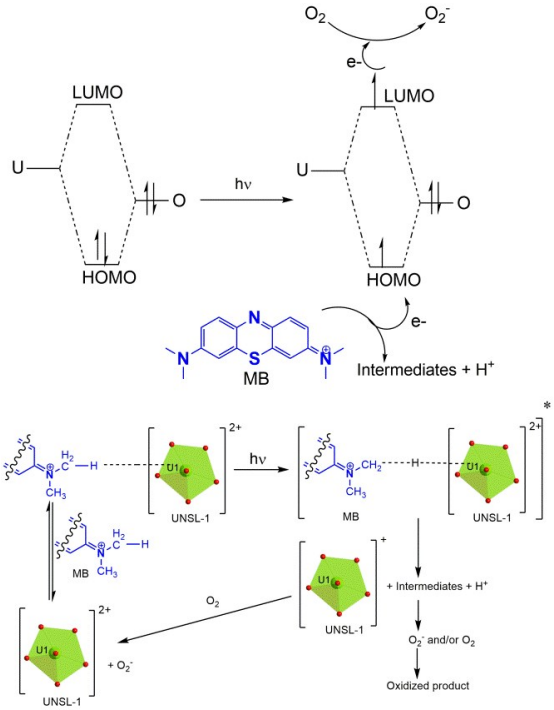

Figure 9. Photocatalytic mechanism of MB degradation in the presence of **UNSL-1** compound.

The uranyl-based materials have a particular photocatalytic mechanism characterized by a process of hydrogen abstraction followed by electron transfer. This process is known as *uranyl-catalyzed photo-oxidation* of organic pollutants.[43] The steps of this mechanism are depicted as follows: $[UO_2]^{2+}$ ions would be excited into highly oxidizing exciting-state $([UO_2]^{+})^*$ under UV light due to LMCT ($U_{5f} \leftarrow O_{2p}$) transition. Both, HOMO (highest occupied molecular orbitals) and LUMO (lowest unoccupied molecular orbitals) are formed by the interaction between U_{5f} and O_{2p} orbitals. The unstable excited electron located in the LUMO will return to the stable HOMO. However, if MB is in an appropriate orientation, the excited $([UO_2]^{2+})^*$ can accept electrons from dyes molecules, giving rise intermediates and protons as products. Also, the excited electrons in the $([UO_2]^{2+})^*$ unit would remain into the LUMO unless it is kept by electronegative substances. Then "LUMO electrons" are captured by O_2 present in the solution in order to generate highly active peroxide anion (O_2^-), which further oxidized and decomposed MB molecules. A summary of the photocatalytic mechanism is depicted in Figure 9.

The band gap-energy between HOMO and LUMO levels of **UNSL-1** was calculated by a diffuse reflectance experiment into the 400-525 nm, resulting in a value of 2.32 eV (see ESI sections 9). The obtained band gap of **UNSL-1** is comparable to other U-MOFs such as $[(UO_2)(DMSO)(p\text{-}MBA)_2]_2$(1) and $[(UO_2)(DMSO)(p\text{-}MBA)_2]_2$(2) with 2.29 and 3.18 eV.[44]

3. Conclusions

A uranyl-coordination polymer based on mixed ligands was successfully obtained under solvothermal synthesis and further characterized by X-ray diffraction techniques. The **UNSL-1** compound with formula $[(UO_2)_2(phen)(succ)_{0.5}(OH)(O)_4(\mu_3\text{-}O)(H_2O)]\cdot H_2O$, crystallizes into the Pī space group. The secondary building unit consists of infinite chains of tetramers connected by succinates. Also, the coordinated phen N-molecules serves as an antenna for bright green light emitter. The photophysical properties were carried out by recording excitation/absorption, emission spectra in aqueous suspension as well as in solid state at 298 K and at 77 K. Moreover, quantification of emitting light was studied by calculating the CIE x,y chromaticity yielding bright green photoluminescence. The emission derived from uranyl LMCT transitions was useful for sensing. For sensing, it was seen a quenching effect in the presence of Fe^{2+} ions, exhibiting a linear response in the range 0-25.5 mM with a LOD of 2.2 mM. Moreover, the compound was tested as an efficient photocatalyst towards MB degradation under sunlight irradiation, producing the dye decomposition in 64 % in 100 minutes.

Finally, it is important to remark the multifunctional profile of the reported material for optics and/or optoelectronic applications, making a contribution to actinide-organic frameworks community.

Conflicts of interest

There are no conflicts to declare.

Acknowledgements

This work was supported by the Consejo Nacional de Investigaciones Científicas y Técnicas, CONICET (PICT-2018-03583, PICT-2016-3017, PIP 820CO) and Universidad Nacional de San Luis (Project PROICO 02-2016). G. E. G., G. E. N, B. B. and G. J. A. A. S. I. are members of Carrera del Investigador Científico (CIC-CONICET). R. D. acknowledges to the Dirección General de Investigaciones from Universidad Santiago de Cali for financial support. J. E. acknowledges the Brazilian funding agency CNPq (grant # 305190/2017-2) for financial support. The authors would like to thank Dra. Paula Angelomé from CNEA, for the TGA measurement.

Table of contents

Graphical Abstract

View Article Online
DOI: 10.1039/D0TC02623A

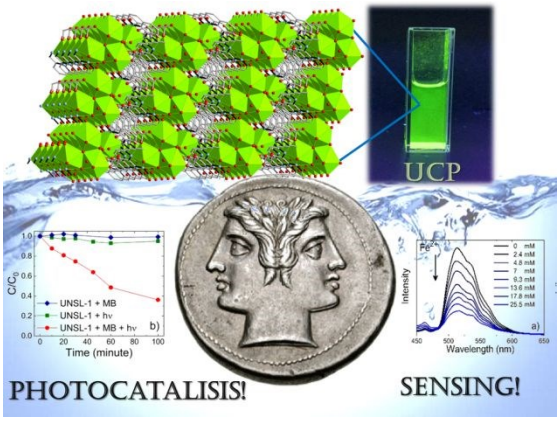

Synopsis: A new mixed uranyl-coordination polymer (UCP) was obtained and applied as strong potential green solid-state lighter for chemical sensing and photocatalyst platform.

[1] (a) C. Xu, G. Tian, S. J. Teat, L. Rao, *Inorg. Chem*., 2013, **52**, 2750; (b) B. Masci, P.Thuéry, *Polyhedron,* 2005, **24**, 229; (c) J. M. Harrowfield, N. Lugan, G. H. Shahverdizadeh, A. A. Soudi, P.Thuéry, *Eur. J. Inorg. Chem*., 2006, **2006**, 389; (d) B. Masci, P. Thuéry, *Cryst. Growth Des.*, 2008, **8**, 1689; (e) P. Thuéry, B. Masci, *Cryst. Growth Des.*, 2010, **10**, 716; (f) Y.-B. Shu, C. Xu, W.-S. Liu, *Eur. J. Inorg. Chem.*, 2013, **2013**, 3592; (g) N. E. Dean, R. D. Hancock, C. L. Cahill, M. Frisch, *Inorg.Chem*., 2008, **47**, 2000; (h) P. Thuéry, B. Masci, *CrystEngComm*, 2012, **14**, 131; (i) R. C. Severance, A. J. Cortese, M. D. Smith, H.-C. zur Loye, *J. Chem. Crystallogr*., 2013, **43**, 171; (j) B. Masci, P. Thuéry, *CrystEngComm*, 2008, **10**, 1082; (k) P. M. Cantos, M. Frisch, C. L. Cahill, *Inorg. Chem. Commun*., 2010, **13**, 1036; (l) M. Frisch, C. L. Cahill, *Dalton Trans*., 2006, 4679; (m) Y. Wang, X. Yin, W. Liu, J. Xie, J. Chen, M. A. Silver, D. Sheng, L. Chen, J. Diwu, N. Liu, Z. Chai, T. E. Albrecht-Schmitt, S. Wang, *Angew. Chem. Int. Ed.,* 2018, **57**, 7883.

[2] (a) W. Yang, T. G. Parker, Z. M. Sun, *Coord. Chem. Rev.,* 2015, **303**, 86. (b) M. B. Andrews, C. L. Cahill, *Chem. Rev.,* 2013, **113**, 1121; (c) K.-X. Wang, J. S. Chen, *Acc. Chem. Res*., 2011, **44**, 531; (d) T. Loiseau, I. Mihalcea, N. Henry, C. Volkringer, *Coord. Chem. Rev*., 2014, **69**, 266; (e) D.-D. Liu, Y.-L. Wang, F. Luo, Q.-Y. Liu, *Inorg. Chem*., 2020, **59**(5), 2952.

[3] G. E. Gomez., A. Ridenour, N. M. Byrne, A. P. Shevchenko, C. L. Cahill, *Inorg. Chem.*, 2019, **58** (11), 7243.

[4] M. C. Bernini, G. E. Gomez, E. V. Brusau, G. E. Narda, *Isr. J. Chem.*, 2018, **58**, 1044.

[5] (a) J.-Y. Kim, A. J. Norquist, Dermot O'Hare, *Dalton Trans*., 2003, **0**, 2813; (b) J. Wang, Z. Wei, F. Guo, C. Li, P.i Zhu, W. Zhu, *Dalton Trans*., 2015, **44**, 13809; (c) S. A. Novikov, M. S. Grigoriev, L. B. Serezhkina, V. N. Serezhkin, *J. Solid State Chem.*, 2017, **248**, 178; (d) Q. L. Guan, F. Ying, B. Yong, H. Xing, J. Liu, H., Z. Zhang, *Inorg. Chem. Comm.,* 2015, **59**, 36.

[6] (a) R. F. D'Vries, G. E. Gomez, J. H. Hodak, G. J. A. A. Soler-Illia, J. Ellena, *Dalton Trans*., 2016, **45**, 646; (b) R. F. D'Vries, G. E. Gomez, D. F. Lionello, M. C. Fuertes, G. J. A. A. Soler-Illia, J. Ellena, *RSC Adv.*, 2016, **6**, 110171.

[7] P. Thuéry, Y. Atoini, J. Harrowfield, *Inorg. Chem*, 2019, **58**, 6550.

[8] (a) Z.-L. Liao, G.-D. Li, M.-H. Bi and J.-S. Chen, *Inorg. Chem*., 2008, **47**, 4844; (b) Z. T. Yu, Z. L. Liao, Y. S. Jiang, G. H. Li and J. S. Chen, *Chem- Eur. J.,* 2005, **11**, 2642; (c) Y.-N. Hou, Y.-H. Xing, F.-Y. Bai, Q.-L. Guan, X. Wang, R. Zhang and Z. Shi, *Spectrochim. Acta, Part A*, 2014, 123, 267; (d) Y. Xia, K.-X. Wang and J.-S. Chen, *Inorg. Chem. Commun.*, 2010, **13**, 1542.

[9] CrysAlisPro *CrysAlisPro*, Agilent Technologies Ltd: Yarnton, Oxfordshire, England, 2014.

[10] G. M. Sheldrick, *Acta Crystallographica Section A,* 2008**, 64** (1), 112.

[11] G. M. Sheldrick, *Acta Crystallographica Section C,* 2015, **71** (1), 3.

[12] L. Farrugia, *J. Appl. Crystallogr.,* 2012**, 45** (4), 849.

[13] Dolomanov, O. V.; Bourhis, L. J.; Gildea, R. J.; Howard, J. A. K.; Puschmann, H., OLEX2: a complete structure solution, refinement and analysis program. *J. Appl. Crystallogr.* **2009,** *42* (2), 339-341.

[14] K. Brandenburg, H. Putz, *DIAMOND- Crystal and Molecular Structure Visualization*, Crystal Impact: Kreuzherrenstr. 102, 53227 Bonn, Germany, 2006.

[15] V. A. Blatov, A. P. Shevchenko, D. M. Proserpio,. *Crystal Growth & Design,* 2014, **14** (7), 3576.

[16] C. F. Macrae, I. J. Bruno, J. A. Chisholm, P. R Edgington, P. McCabe, E. Pidcock, L. Rodriguez-Monge, R. Taylor, J. Van De Streek, P. A. Wood, *J. Appl. Crystallogr*., 2008, **41** (2), 466.

[17] Onna, D., Fuentes, K. M., Spedalieri, C., Perullini, M., Marchi, M. C., Alvarez, F., & Bilmes, S. A. (2018). Wettability, Photoactivity, and Antimicrobial Activity of Glazed Ceramic Tiles Coated with Titania Films Containing Tungsten. ACS Omega, 3(12), 17629-17636.

[18] Connelly, N. G., ; Damhus, T.;Hartshorn, R.M.; Hutton, A.T., *Nomenclature of Inorganic Chemistry - IUPAC Recommendations 2005*. RSC Publishing: Cambridge, UK., 2005; p 377.

[19] M. C. Bernini, E. V. Brusau, G. E. Narda, G. Echeverria, A. Fantoni, G. Punte, A. P. Ayala, *Polyhedron*, 2012, **31**, 729.

[20] A. K. Cheetham, C. N. R. Rao, R. K. Feller, *Chem. Comm*., 2006, 4780.

[21] (a) P .Li, N. A. Vermeulen, X. Gong, C. D. Malliakas, J. F. Stoddart, J. T. Hupp, O. K. Farha, *Angew. Chem*., 2016, **128**, 10514; (b) K. S. Park, Z. Ni, A. P. Côté, J. Y. Choi, R. Huang, F. J. Uribe-Romo, H. K. Chae, M. O'Keeffe, O. M. Yaghi, *Proc. Natl. Acad. Sci. U. S. A*. 2006, **103**, 10186.

[22] J. Heine, K. Müller-Buschbaum, *Chem. Soc. Rev.,* 2013, **42**, 9232.

[23] R. G. Denning, *J. Phys. Chem. A*, 2007, **111**, 4125.

View Article Online
DOI: 10.1039/D0TC02623A

[24] P. Thuéry, J. Harrowfield, *Cryst. Growth Des*., 2014, **14**, 1314.
[25] J.T. Bell, R.E. Biggers, *J. Mol. Spectrosc*. 1965, **18**, 247.
[26] J.T. Bell, R.E. Biggers, *J. Mol. Spectrosc*. 1967, **22**, 262.
[27] J.T. Bell, R.E. Biggers, *J. Mol. Spectrosc*. 1968, **25**, 312.
[28] S. V. Eliseeva, J.-C. G. Bünzli, *Chem. Soc. Rev*., **2010**, 39, 189.
[29] K. P. Carter, C. H. F. Zulato, C. L. Cahill, *CrystEngComm*, 2014, **16**, 10189.
[30] S. G. Thangavelu, M. B. Andrews, S. J. A. Pope, C. L. Cahill, *Inorg. Chem*., 2013, **52**, 2060.
[31] (a) Y. Cui, H. Xu, Y. Yue, Z. Guo, J. Yu, Z. Chen, J. Gao, Y. Yang, G. Qian, B. Chen, *J. Am. Chem. Soc*., 2012, **134**, 3979; (b) R. F. D'Vries, S. Álvarez-García, N. Snejko, L. E. Bausá, E. Gutiérrez-Puebla, A. de Andrés, M. A. Monge, *J. Mater. Chem. C*, 2013, **1**, 6316.
[32] (a) G. E. Gomez, A. M. Kaczmarek, R. Van Deun, E. V. Brusau, G. E. Narda, D. Vega, M. Iglesias, E. Gutierrez-Puebla, M. Ángeles Monge. *Eur. J. Inorg. Chem*., 2016, **2016**, 1577; (b) A. A. Godoy, G. E. Gomez, A. M. Kaczmarek, R. Van Deun, O. J. Furlong, F. Gándara, M. A. Monge, M. C. Bernini, G. E. Narda, *J. Mater. Chem. C*, 2017, **5**, 12409.
[33] Z. Hu, B. J. Deibert, J. Li, *Chem. Soc. Rev*., 2014, **43**, 5815.
[34] G. E. Gomez, M. dos Santos Afonso, H.A. Baldoni, F. Roncaroli, G. J. A. A. Soler-Illia, *Sensors*, 2019, **19**, 1260.
[35] R. F. D'Vries, G. E. Gomez, L. Paola Mondragon, D. Onna, B. C. Barja, G. J. A. A. Soler-Illia, J. Ellena, *J. Solid State Chem*., 2019, **274**, 322.
[36] Pham, A. N., & Waite, T. D. (2008). *Geochimica et Cosmochimica Acta*, **72**(**15**), 3616-3630.
[37] Fontana, I., Lauria, A., & Spinolo, G. (2007). *Physica status solidi (b)*, 244(12), 4669-4677.
[38] Moriyasu, M., Yokoyama, Y., & Ikeda, S. (1977). *Journal of Inorganic and Nuclear Chemistry*, 39(12), 2205-2209.
[39] Matsushima, R., Fujimori, H., & Sakuraba, S. (1974). Journal of the Chemical Society, Faraday Transactions 1: Physical Chemistry in Condensed Phases, 70, 1702-1709.
[40] Lakowicz, J. R. (Ed.). (2013). Principles of fluorescence spectroscopy. Springer Science & Business Media.
[41] P. Wu, J. Wang, Y. Li, C. He, Z. Xie, C. Duan, *Adv. Funct. Mater*., 2011, **21**, 2788.
[42] Z.-T. Yu, Z.-L. Liao, Y.-S. Jiang, G.-H. Li, G.-D. Li, J.-S., Chen, *Chem. Comm*., 2004, 1814.
[43] D. Li, W.-D. Shi, *Chin. J. Catal*. 37 (2016) 792.
[44] X.-S. Zhai, Y. –Q. Zheng, J.-Li Lin, W. Xu, *Inorg. Chim. Acta*, 2014, **423**, 1.